

Enhancing dynamic range through quantum deamplification

Qi Liu,^{1,*} Ming Xue,^{2,*} Xinwei Li,³ Denis V. Vasilyev,⁴ and Ling-Na Wu^{5,†}

¹*Department of Physics, MIT-Harvard Center for Ultracold Atoms and Research Laboratory of Electronics, Massachusetts Institute of Technology, Cambridge, Massachusetts 02139, USA*

²*Department of Physics & Key Laboratory of Aerospace Information Materials and Physics, Nanjing University of Aeronautics and Astronautics, Nanjing 211106, China*

³*Beijing Academy of Quantum Information Sciences, Xibeiwang East Road, Beijing 100193, China*

⁴*Institute for Theoretical Physics, University of Innsbruck, 6020 Innsbruck, Austria*

⁵*Center for Theoretical Physics & School of Physics and Optoelectronic Engineering, Hainan University, Haikou 570228, China*

(Dated: December 20, 2024)

Balancing high sensitivity with a broad dynamic range (DR) is a fundamental challenge in measurement science, as improving one often compromises the other. While traditional quantum metrology has prioritized enhancing local sensitivity, a large DR is crucial for applications such as atomic clocks, where extended phase interrogation times contribute to wider phase range. In this Letter, we introduce a novel quantum deamplification mechanism that extends DR at a minimal cost of sensitivity. Our approach uses two sequential spin-squeezing operations to generate and detect an entangled probe state, respectively. We demonstrate that the optimal quantum interferometer limit can be approached through two-axis counter-twisting dynamics. Further expansion of DR is possible by using sequential quantum deamplification interspersed with phase encoding processes. Additionally, we show that robustness against detection noise can be enhanced by a hybrid sensing scheme that combines quantum deamplification with quantum amplification. Our protocol is within the reach of state-of-the-art atomic-molecular-optical platforms, offering a scalable, noise-resilient pathway for entanglement-enhanced metrology.

Introduction.— In the field of precision measurement, achieving high sensitivity to the signal of interest across a broad measurement range is a key goal [1–3]. Considerable advancements have been made in surpassing the standard quantum limit (SQL)—the best phase sensitivity achievable with uncorrelated particles—by leveraging entangled probe states, including squeezed states [4–18], Dicke states [19–23], and Schrödinger-cat-like states [24–29]. However, the enhanced sensitivity obtained in this way is usually confined to a narrow phase range [30–32]. Moreover, the detection of entangled states is susceptible to technical noise, which diminishes the theoretical metrological benefits promised by entanglement [33, 34]. To address the latter challenge, quantum amplification (QA) techniques [35–41] have been developed. These methods typically amplify the signal through squeezing-unsqueezing protocols [14, 42–45]. The introduction of unsqueezing, however, comes with the trade-off of an even more limited phase range within which beyond-SQL sensitivity can be achieved [14, 46].

While the emphasis has predominantly been on boosting local sensitivity, the demand for a broad measurement range in practical applications is equally important and warrants greater attention. Previous studies have shown that by using auxiliary interferometers, one can enhance the dynamic range (DR), within which the phase can be extracted from the measurement unambiguously. For instance, employing dual-quadrature measurement with two ensembles doubles DR [47, 48]. Even greater enhancement in DR is possible through the use of multiple ensembles with different interrogation phases [49–53]. By integrating these techniques with entangled states, it is possible to achieve beyond-SQL phase sensitivity across an extended phase range [25, 26, 48, 54–56]. The ultimate goal is to optimize both estimation precision

and DR by leveraging quantum resources native to the experimental platform. This can be achieved via quantum variational optimization, which designs quantum circuits generating optimal input states and measurements that minimize the Bayesian mean squared error for a given prior distribution of a parameter [30, 57]. Experimental implementations [58] of such circuits approach the performance of an optimal quantum interferometer (OQI) but face increasing circuit complexity as system size grows. The challenge lies in identifying quantum sensing protocols and resources that enable simple, robust circuits capable of nearing OQI performance despite experimental imperfections.

In this paper, we introduce a novel mechanism that leverages *quantum deamplification* (QD) to extend DR using a single ensemble in the presence of detection noise. Unlike the QA protocols [35, 42, 45], our method employs two sequential squeezing stages to deamplify the encoded phase at a minimal cost of local sensitivity, thereby achieving a broader DR. We demonstrate this mechanism by using a generalized Ramsey interferometer based on two-axis counter-twisting (TACT) interaction [4, 59, 60], which is both efficient in generating spin squeezing and particularly elegant for illustrating the core idea of our approach. This method approaches the OQI limit [30, 61] in sensing performance using only one TACT gate each for state preparation and measurement. Furthermore, interspersing phase encoding with TACT squeezing—progressively deamplifying the signal—expands DR further, albeit with reduced local sensitivity, bringing the overall single-shot sensing performance closer to the OQI limit. To enhance noise robustness, we propose a hybrid sensing protocol combining QD, QA, and adaptive one-way local operations and classical communication (LOCC) measurements [62], enabling high-sensitivity phase estimation over a

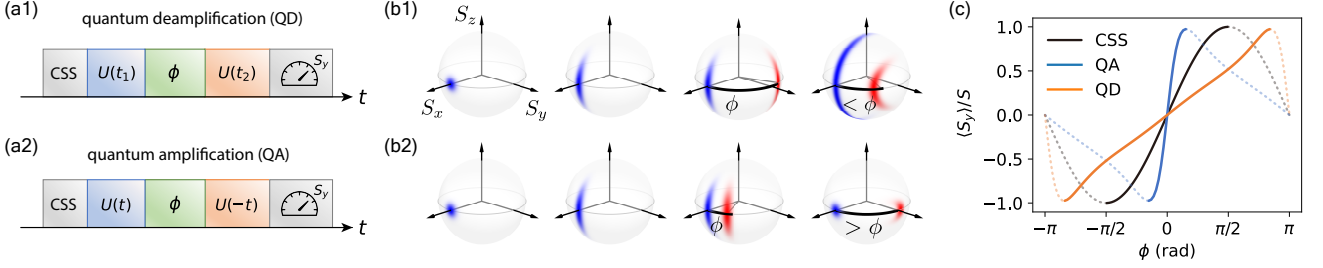


Figure 1. (a1-a2) Schematics of interferometry based on quantum deamplification (QD) and amplification (QA). (b1-b2) Husimi representations of states during QD and QA. The blue (red) shading denotes the state without (with) phase encoding. The phase encoded on a spin squeezed state results in variations of $\langle S_y \rangle$, which gets deamplified (amplified) after a subsequent squeezing (unsqueezing) process. (c) Normalized spin observable $\langle S_y \rangle/S$ as a function of phase ϕ . Coherent spin state (CSS) provides a DR around $[-\pi/2, \pi/2]$ (black solid line), within which the phase can be distinguished unambiguously. Signal deamplification extends this range to nearly $[-\pi, \pi]$ (orange solid line), while signal amplification further narrows the DR (blue solid line). Calculations are implemented in the TACT model with $N = 100$.

wide DR despite experimental imperfections.

Quantum (de)amplification.— We consider estimation of the phase ϕ in an atomic interferometer consisting of N identical two-level atoms. For a classical probe in the coherent spin state (CSS), measurement precision is inherently bounded by the SQL, $1/\sqrt{N}$. The DR is confined to $[-\pi/2, \pi/2]$, since ϕ and $\pm\pi - \phi$ yield the same measurement outcome [black curve in Fig. 1(c)]. In the QA protocol, which involves a squeezing-encoding-unsqueezing sequence as shown in Fig. 1(a2), the encoded signal is amplified. Since the amplified phase can only be distinctly resolved within $[-\pi/2, \pi/2]$, the encoded phase ϕ to be estimated is further restricted, as depicted by the blue curve in Fig. 1(c) with a steeper gradient near small phases and a more limited DR. In contrast to QA, we propose to introduce a second squeezing process before measurement, which serves to deamplify the signal (Fig. 1(a1)). Given that the encoded phase ϕ exceeds the deamplified phase, and the latter is confined to the range of $[-\pi/2, \pi/2]$, this mechanism enables the unambiguous estimation of phase ϕ that extends beyond the classical boundaries of $[-\pi/2, \pi/2]$, as shown by the orange curve in Fig. 1(c).

Dual-TACT-interacting protocol.— Building on the above discussion, we now delve into a more detailed examination of our proposal. We employ the TACT squeezing model [4], governed by the Hamiltonian $\hat{H}_{\text{TACT}} = \chi(\hat{S}_y\hat{S}_z + \hat{S}_z\hat{S}_y)$ with interaction strength χ , where $\hat{S}_{x,y,z} = \sum_{k=1}^N \hat{\sigma}_{x,y,z}^{(k)}/2$ are the collective spin operators and $\hat{\sigma}_{x,y,z}^{(k)}$ the Pauli operators for the k -th atom. Recent experiments have successfully demonstrated the mean-field spin dynamics of the TACT model in cavity-QED systems [59] and within the realm of ultracold polar molecules [60], making the observation of spin squeezing highly promising in the near future. The structure of our dual-TACT-interacting quantum interferometer is shown in Fig. 2(a). It begins with a CSS as the initial state $|\Psi_0\rangle$, followed by the application of the TACT interaction twice [also cf. Fig. 1(a)]. The first instance of TACT interaction precedes the phase encoding process, serving to prepare an entangled probe state, while the second application takes place

after phase encoding, facilitating nonlinear readout. The encoded phase is inferred from the collective spin \hat{S}_y through projective measurements.

The phase estimation accuracy is characterized by the mean squared error (MSE) with respect to the actual phase ϕ , $\epsilon(\phi) = \sum_m [\phi - \phi_{\text{est}}(m)]^2 p(m|\phi)$, where $p(m|\phi)$ denotes the conditional probability of measurement outcome m , and is given by $p(m|\phi) = |\langle m|\hat{U}(t_2)e^{-i\phi\hat{S}_z}\hat{U}(t_1)|\Psi_0\rangle|^2$, with $|m\rangle \equiv |S = N/2, S_y = m\rangle$ being the eigenstate of \hat{S}_y with eigenvalue m . Here, $\hat{U}(t) = e^{-i\hat{H}_{\text{TACT}}t}$, and t_1, t_2 represent the evolution time parameters for the two TACT segments. The optimal values of t_1 and t_2 are to be found through optimization. We assume a linear estimator $\phi_{\text{est}}(m) = am$, and the optimal a is determined from the measurement outcome distribution [57]. Our goal is to achieve optimal sensitivity for phase ϕ in a prior phase range $\delta\phi$. Assuming a Gaussian prior phase distribution centered at zero, $\mathcal{P}_{\delta\phi}(\phi) = \exp[-\phi^2/(\sqrt{2}\delta\phi)^2]/\sqrt{2\pi(\delta\phi)^2}$, we minimize the MSE averaged over the prior distribution, defining the Bayesian mean squared error (BMSE): $(\Delta\phi)^2 = \int d\phi \epsilon(\phi)\mathcal{P}_{\delta\phi}(\phi)$.

Figure 2 showcases the performance of our TACT-based quantum interferometer, benchmarked against the classical Ramsey interferometer, the OQI, and a setup utilizing TACT interaction solely for probe state preparation. In the last scenario, the interaction time is also optimized to minimize the BMSE. In Fig. 2(b), we depict the posterior uncertainty $\Delta\phi$, normalized by the prior uncertainty $\delta\phi$, as a function of $\delta\phi$ for these various configurations. This quantity is related to frequency stability in atomic clock, characterized by Allan deviation [58, 63]. A smaller value of $\Delta\phi/\delta\phi$ indicates a lower phase estimation error (smaller $\Delta\phi$) over a broader phase range (larger $\delta\phi$). For all cases, $\Delta\phi/\delta\phi$ initially declines as $\delta\phi$ grows and then starts to rise due to increase probability of phase slip error [30, 34, 57]. When compared to the classical Ramsey interferometer (black line, CSS), the use of TACT interaction for probe state preparation alone (blue line, SSS), enhances sensitivity at small $\delta\phi$ values. However, this improvement diminishes as $\delta\phi$ grows, due to the fact that SSS

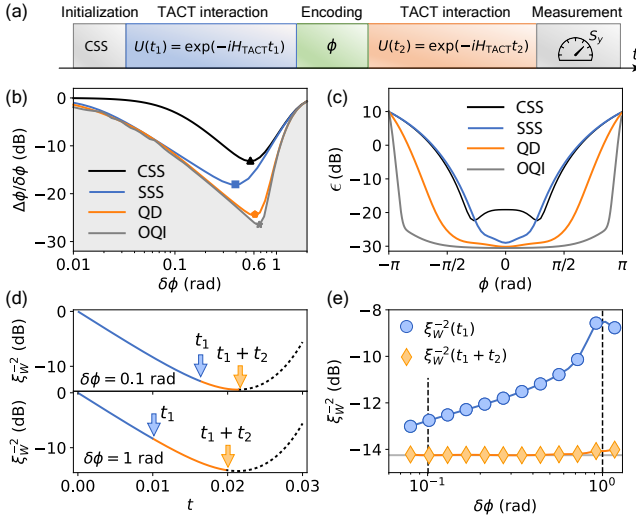


Figure 2. Dual-TACT-interacting protocol. (a) The protocol sequence starts from a coherent spin state (CSS) along x direction which evolves to a spin squeezed state (SSS) under TACT evolution $U(t_1)$. After a phase (ϕ) encoding operation, $U(t_2)$ deamplifies the signal before the final measurement of \hat{S}_z . (b) Optimized sensor performance, characterized by $\Delta\phi/\delta\phi$, for sensing schemes with CSS (black line), SSS (blue line), and quantum deamplification (QD, orange line) at various prior phase uncertainties $\delta\phi$. The grey region denotes the inaccessible regime, bounded by the OQI limit (grey line). Markers highlight the best performance (minima) at the turning point. (c) Mean square error of the sensing schemes, evaluated at $\delta\phi$ and TACT squeezing times corresponding to the minima of $\Delta\phi/\delta\phi$ in (b). (d) TACT-interacting times t_1 (blue) and t_2 (orange) and their corresponding squeezing parameters evolution, for two selected $\delta\phi$ marked by dashed vertical lines in (e). (e) Squeezing parameters for the $\delta\phi$ -dependent optimal probe (blue circles) and final state (orange diamonds) in the QD scheme. The horizontal grey line marks the optimal spin squeezing obtainable with TACT interaction. All calculations in this paper assume $N = 100$ and $\chi = 1$.

only promises beyond-SQL phase sensitivity within a narrow phase range. Incorporating a second TACT interacting process post phase encoding (orange curve) significantly enhances the precision of phase estimation at large $\delta\phi$. Notably, its performance nearly approaches the theoretical limit given by the OQI (grey curve) with the optimal probe state and measurement.

Figure 2(c) displays the MSE as a function of the phase ϕ . The prior uncertainties $\delta\phi$ and TACT squeezing times are selected to achieve the minimal $\Delta\phi/\delta\phi$ as indicated by the markers in panel (b). It is evident that the interferometer employing SSS surpasses the classical interferometer at small ϕ . The dual-TACT-interacting protocol (orange line) further diminishes the error across the entire $[-\pi, \pi]$ range.

The superior performance of the dual-TACT-interacting protocol can be credited to the aforementioned squeezing-squeezing mechanism which allows for an extended DR. This is clearly demonstrated in Fig. 2(d), which shows the evolution of the system's squeezing degree for two distinct $\delta\phi$. The squeezing degree is quantified by the Wineland param-

eter [64, 65], $\xi_W^2 = N\Delta^2\hat{S}_{\perp,\min}/|\langle\hat{\mathbf{S}}\rangle|^2$, where $\Delta^2\hat{S}_{\perp,\min}$ denotes the minimal spin fluctuation on the plane perpendicular to the mean spin direction and the collective spin vector $\hat{\mathbf{S}} = (\hat{S}_x, \hat{S}_y, \hat{S}_z)$. Figure 2(d) reveals a sequential squeezing process, where the initial squeezing (blue segment) creates a SSS used as a probe, while the subsequent squeezing (orange segment), leads to signal deamplification, thereby enhancing the DR. An overview of the squeezing parameter as a function of $\delta\phi$ is shown in Fig. 2(e). One can see that the squeezing of the probe state (blue) is always less pronounced than that of the final state (orange). Particularly, the final state is close to the optimal squeezed state. In other words, the journey to the optimal squeezed state is divided into two segments, one for state preparation and the other for signal deamplification. The timing for phase encoding, nestled between these two processes, depends on the prior phase uncertainty: for a broader prior distribution (larger $\delta\phi$), phase encoding should occur earlier to maximize the signal deamplification effect, as shown in Fig. 2(d).

Sequential QD interspersed with phase encoding.—Given the cyclical nature of phase—where ϕ and $\phi + 2\pi$ are indistinguishable—the maximum DR of the aforementioned methodologies is inherently restricted to the interval $[-\pi, \pi]$. To surmount this limitation, we advocate the implementation of sequential QD. As illustrated in Fig. 3(a), this approach involves the iterative application of spin squeezing interspersed with phase encoding, which, in the limit of infinite iterations, approaches to concurrent entanglement generation and phase interrogation [66, 67]. This methodical layering of phase encoding and TACT interaction serves to deamplify the signal progressively [Fig. 3(b)], thereby extending the DR beyond $[-\pi, \pi]$. In Fig. 3(c), the estimated phase ϕ_{est} is depicted as a

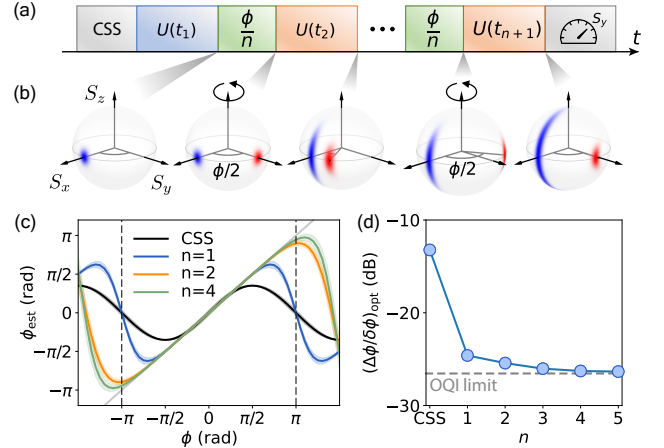


Figure 3. (a) Schematics of the sequential QD interspersed with phase encoding. (b) Evolution of quantum state on the Bloch spheres for $n = 2$. (c) Estimated phase ϕ_{est} as a function of the real phase ϕ . The shading represents the square root of the MSE. The grey solid line denotes the unbiased estimation with $\phi_{\text{est}} = \phi$. (d) Optimal $\Delta\phi/\delta\phi_{\text{opt}}$ as a function of n . The OQI limit is illustrated by the grey dashed line.

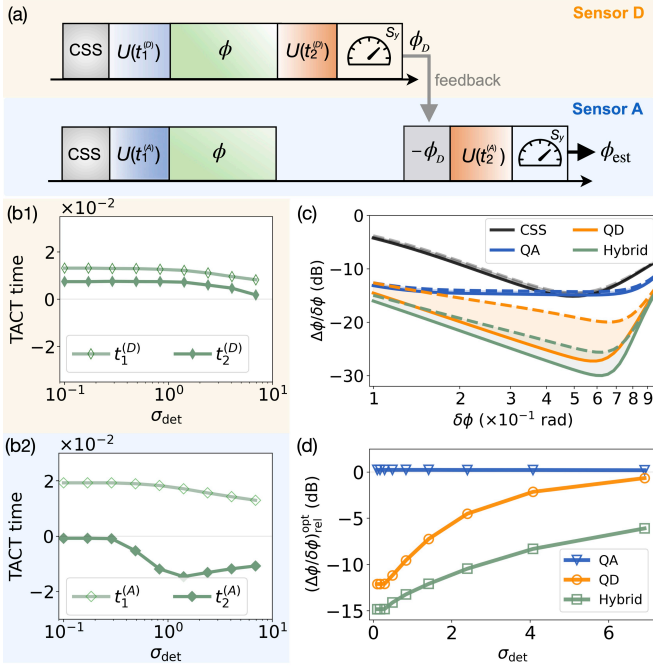


Figure 4. Hybrid sensing with adaptive measurement. (a) Two sensors are conjointly used for measuring the phase of LO. The phase estimated from the sensor D is subtracted from the phase encoded on sensor A. (b) The optimal TACT-interacting times for the two sensors as a function of detection noise. (c) Optimized $\Delta\phi/\delta\phi$ for various sensing schemes. The solid (dashed) curves denote the results in the absence (presence, with $\sigma_{\text{det}} = 2$) of detection noise. (d) The minimal phase estimation error with respect to the classical Ramsey interferometric sensor, $(\Delta\phi/\delta\phi)_{\text{rel}}^{\text{opt}} \equiv (\Delta\phi/\delta\phi)^{\text{opt}}/(\Delta\phi/\delta\phi)_{\text{CSS}}^{\text{opt}}$, as a function of detection noise σ_{det} .

function of the encoded phase ϕ , across various order n . The ideal estimation is unbiased, aligning ϕ_{est} with ϕ , as indicated by the grey solid line. One can see that with each additional layer of phase encoding, the unambiguous phase estimation regime is enhanced. The sequential QD also brings the benefit of reducing BMSE as shown in Fig. 3(d), which converges to the OQI limit.

Hybrid sensing with adaptive measurement.— In the absence of detection noise, the QD sensor is capable of reaching the OQI performance, providing a near-optimal balance between the local sensitivity and phase sensing range. However, the QD sequence ends up with an extremely squeezed state before measurement, which renders the metrological performance susceptible to detection noise. This challenge also exists in the circuit optimization for a generalized Ramsey interferometers [30, 57], and poses one practical limitation of the latter in large systems. In contrast, QA sensor exhibits strong resilience to detection noise, though this robustness comes at the expense of a narrower DR. Here we study an *hybrid sensing* scheme [63] to harness the complementary strengths of these two sensors in a synergistic manner. The QD sensor, with its ability to offer a broad DR is utilized for the initial phase detection. It allows for the sensing process to effectively

handle a variety of phase shifts, although the sensitivity would be compromised by detection noise. To address this, we then employ the QA sensor with an *adaptive* measurement to refine the phase estimation, improving the system’s resilience to noise and reducing the phase estimation error.

To validate our idea numerically, we design a hybrid system comprising two TACT-based sensors interrogated with the same local oscillator (LO), as shown in Fig. 4(a). The first sensor (D) provides an initial estimate of the LO phase ϕ , called ϕ_D . This phase estimate is fed back to the second sensor (A) by adjusting the control pulse phase, effectively adding $-\phi_D$ to the interrogation phase ϕ . Finally, by analyzing its output to get ϕ_A , we estimate the phase ϕ as $\phi_{\text{est}} = \phi_D + \phi_A$.

We optimize the TACT-interacting times at two stages—before and after the phase encoding—in both sensors, $\{t_1^{(D)}, t_2^{(D)}, t_1^{(A)}, t_2^{(A)}\}$, with the goal of minimizing the BMSE in the presence of detection noise σ_{det} [68]. The results, depicted in Fig. 4(b), illustrate how these interaction times vary with the level of detection noise. The interaction times for the first sensor are both positive, signifying its role as a QD sensor with a sequential squeezing process. On the other hand, the second sensor exhibits a positive interaction time prior to phase encoding ($t_1^{(D)} > 0$) and a negative interaction time post phase encoding ($t_2^{(D)} < 0$), which is indicative of a QA sensor with a squeezing-unsqueezing mechanism.

In Fig. 4(c), we compare the BMSE of the hybrid sensor with several individual sensing schemes. To guarantee a fair comparison, we employ the same total number of particles in all the schemes [69]. The solid (dashed) curves denote the results in the absence (presence, with $\sigma_{\text{det}} = 2$) of detection noise. Among the individual sensing schemes (either split into two independent sensors of N atoms or measured independently twice with N atoms), the QA sensor (blue curves) exhibits strong resilience to detection noise (highlighted by the shading area), while it falls short in BMSE. In contrast, the QD sensor (orange curves) provides a small phase estimation error over a broad range of $\delta\phi$, but is highly susceptible to detection noise. The hybrid sensor (green curves), which combines the strengths of both QD and QA sensors, demonstrates robustness against detection noise and maintains low phase estimation error across a broad range of phase. Figure 4(d) further highlights the resilience difference between the sensors. One can see that the hybrid sensor (green curve) consistently outperforms the other sensors across all levels of detection noise, and its performance degrades slower with increasing detection noise compared to the individual QD sensor.

Conclusion— We introduce a novel QD mechanism leveraging the TACT interaction to extend the DR of phase measurements. The phase encoded on the squeezed state gets deamplified during the second squeezing stage at a minimal cost of local sensitivity, thereby achieving a broader DR and approaching the OQI limit. This scheme is further enhanced by sequential QD interspersed with multiple

phase encoding processes. Since the QD sequence ends in an extremely squeezed state before measurement, its metrological performance becomes highly susceptible to detection noise. To address this limitation, we propose a hybrid sensing scheme that combines the advantages of both QD and QA sensors. Our method thus represents a promising advancement in entanglement-enhanced metrology, with the potential to significantly improve applications such as the long-term stability of atomic clocks and other precision measurement systems [70].

Acknowledgement. We thank Vladan Vuletić, Leon Zaporski, Gustavo Velez, Matthew Radzihovsky, Guo-Qing Wang and Zhi-Yao Hu for helpful discussion. This work is supported by the National Natural Science Foundation of China (Grant No. 12304543) and the Innovation Program for Quantum Science and Technology (Grant No. 2021ZD0302100). L.-N.W. acknowledges support by the Hainan Province Science and Technology Talent Innovation Project (Grant No. KJRC2023L05). D.V.V. acknowledges funding by the Austrian Science Fund (FWF) [10.55776/COE1]. M.X. is also supported by the Jiangsu Province & Longcheng Youth Science and Technology Talent Support Project.

* These authors contributed equally to this work.

† lingna.wu@hainanu.edu.cn

- [1] C. L. Degen, F. Reinhard, and P. Cappellaro, Quantum sensing, *Rev. Mod. Phys.* **89**, 035002 (2017).
- [2] L. Pezzè, A. Smerzi, M. K. Oberthaler, R. Schmied, and P. Treutlein, Quantum metrology with nonclassical states of atomic ensembles, *Rev. Mod. Phys.* **90**, 035005 (2018).
- [3] J. Huang, M. Zhuang, and C. Lee, Entanglement-enhanced quantum metrology: From standard quantum limit to heisenberg limit, *Applied Physics Reviews* **11**, 031302 (2024).
- [4] M. Kitagawa and M. Ueda, Squeezed spin states, *Phys. Rev. A* **47**, 5138 (1993).
- [5] A. Kuzmich, K. Mølmer, and E. S. Polzik, Spin squeezing in an ensemble of atoms illuminated with squeezed light, *Phys. Rev. Lett.* **79**, 4782 (1997).
- [6] J. Hald, J. L. Sørensen, C. Schori, and E. S. Polzik, Spin squeezed atoms: A macroscopic entangled ensemble created by light, *Phys. Rev. Lett.* **83**, 1319 (1999).
- [7] C. Gross, T. Zibold, E. Nicklas, J. Estève, and M. K. Oberthaler, Nonlinear atom interferometer surpasses classical precision limit, *Nature* **464**, 1165 (2010).
- [8] M. F. Riedel, P. Böhi, Y. Li, T. W. Hänsch, A. Sinatra, and P. Treutlein, Atom-chip-based generation of entanglement for quantum metrology, *Nature* **464**, 1170 (2010).
- [9] L. Pezzè and A. Smerzi, Ultrasensitive two-mode interferometry with single-mode number squeezing, *Phys. Rev. Lett.* **110**, 163604 (2013).
- [10] R. Schmied, J.-D. Bancal, B. Allard, M. Fadel, V. Scarani, P. Treutlein, and N. Sangouard, Bell correlations in a bose-einstein condensate, *Science* **352**, 441 (2016).
- [11] E. S. Polzik and J. Ye, Entanglement and spin squeezing in a network of distant optical lattice clocks, *Phys. Rev. A* **93**, 021404 (2016).
- [12] J. G. Bohnet, B. C. Sawyer, J. W. Britton, M. L. Wall, A. M. Rey, M. Foss-Feig, and J. J. Bollinger, Quantum spin dynamics and entanglement generation with hundreds of trapped ions, *Science* **352**, 1297 (2016).
- [13] S. Colombo, E. Pedrozo-Peñañiel, and V. Vuletić, Entanglement-enhanced optical atomic clocks, *Applied Physics Letters* **121** (2022).
- [14] T.-W. Mao, Q. Liu, X.-W. Li, J.-H. Cao, F. Chen, W.-X. Xu, M. K. Tey, Y.-X. Huang, and L. You, Quantum-enhanced sensing by echoing spin-nematic squeezing in atomic bose-einstein condensate, *Nature Physics* **19**, 1585 (2023).
- [15] G. P. Greve, C. Luo, B. Wu, and J. K. Thompson, Entanglement-enhanced matter-wave interferometry in a high-finesse cavity, *Nature* **610**, 472 (2022).
- [16] D. Ganapathy, W. Jia, M. Nakano, and et al (LIGO O4 Detector Collaboration), Broadband quantum enhancement of the ligo detectors with frequency-dependent squeezing, *Phys. Rev. X* **13**, 041021 (2023).
- [17] W. Jia, V. Xu, K. Kuns, and et al, Squeezing the quantum noise of a gravitational-wave detector below the standard quantum limit, *Science* **385**, 1318 (2024).
- [18] J. M. Robinson, M. Miklos, Y. M. Tso, C. J. Kennedy, T. Bothwell, D. Kedar, J. K. Thompson, and J. Ye, Direct comparison of two spin-squeezed optical clock ensembles at the 10^{-17} level, *Nature Physics* **20**, 208 (2024).
- [19] S. F. Huelga, C. Macchiavello, T. Pellizzari, A. K. Ekert, M. B. Plenio, and J. I. Cirac, Improvement of frequency standards with quantum entanglement, *Phys. Rev. Lett.* **79**, 3865 (1997).
- [20] B. Lücke, M. Scherer, J. Kruse, L. Pezzè, F. Deuretzbacher, P. Hyllus, O. Topic, J. Peise, W. Ertmer, J. Arlt, L. Santos, A. Smerzi, and C. Klempt, Twin matter waves for interferometry beyond the classical limit, *Science* **334**, 773 (2011).
- [21] Z. Zhang and L. M. Duan, Quantum metrology with dicke squeezed states, *New Journal of Physics* **16**, 103037 (2014).
- [22] X.-Y. Luo, Y.-Q. Zou, L.-N. Wu, Q. Liu, M.-F. Han, M. K. Tey, and L. You, Deterministic entanglement generation from driving through quantum phase transitions, *Science* **355**, 620 (2017).
- [23] Y.-Q. Zou, L.-N. Wu, Q. Liu, X.-Y. Luo, S.-F. Guo, J.-H. Cao, M. K. Tey, and L. You, Beating the classical precision limit with spin-1 dicke states of more than 10,000 atoms, *Proceedings of the National Academy of Sciences* **115**, 6381 (2018).
- [24] T. Chalopin, C. Bouazza, A. Evrard, V. Makhlov, D. Dreon, J. Dalibard, L. A. Sidorenkov, and S. Nascimbene, Quantum-enhanced sensing using non-classical spin states of a highly magnetic atom, *Nature Communications* **9**, 4955 (2018).
- [25] A. Cao, W. J. Eckner, T. Lukin Yelin, A. W. Young, S. Jandura, L. Yan, K. Kim, G. Pupillo, J. Ye, N. Darkwah Oppong, *et al.*, Multi-qubit gates and schrödinger cat states in an optical clock, *Nature* **634**, 315 (2024).
- [26] R. Finkelstein, R. B.-S. Tsai, X. Sun, P. Scholl, S. Direkci, T. Gefen, J. Choi, A. L. Shaw, and M. Endres, Universal quantum operations and ancilla-based read-out for tweezer clocks, *Nature* **634**, 321 (2024).
- [27] T. Kielinski, P. O. Schmidt, and K. Hammerer, GHZ protocols enhance frequency metrology despite spontaneous decay, *Science Advances* **10**, eadr1439 (2024).
- [28] Y. A. Yang, W. T. Luo, J. L. Zhang, S. Z. Wang, C.-L. Zou, T. Xia, and Z. T. Lu, Minute-scale schrödinger-cat state of spin-5/2 atoms, *Nature Photonics* [10.1038/s41566-024-01555-3](https://doi.org/10.1038/s41566-024-01555-3) (2024).
- [29] X. Zhang, Z. Hu, and Y.-C. Liu, Fast generation of ghz-like states using collective-spin XYZ model, *Phys. Rev. Lett.* **132**, 113402 (2024).

- [30] R. Kaubruegger, D. V. Vasilyev, M. Schulte, K. Hammerer, and P. Zoller, Quantum variational optimization of ramsley interferometry and atomic clocks, *Phys. Rev. X* **11**, 041045 (2021).
- [31] R. Kaubruegger, A. Shankar, D. V. Vasilyev, and P. Zoller, Optimal and variational multiparameter quantum metrology and vector-field sensing, *PRX Quantum* **4**, 020333 (2023).
- [32] D. V. Vasilyev, A. Shankar, R. Kaubruegger, and P. Zoller, [Optimal multiparameter metrology: The quantum compass solution \(2024\)](#), [arXiv:2404.14194 \[quant-ph\]](#).
- [33] A. André, A. S. Sørensen, and M. D. Lukin, Stability of atomic clocks based on entangled atoms, *Phys. Rev. Lett.* **92**, 230801 (2004).
- [34] M. Schulte, C. Lisdat, P. O. Schmidt, U. Sterr, and K. Hammerer, Prospects and challenges for squeezing-enhanced optical atomic clocks, *Nature Communications* **11**, 5955 (2020).
- [35] E. Davis, G. Bentsen, and M. Schleier-Smith, Approaching the heisenberg limit without single-particle detection, *Phys. Rev. Lett.* **116**, 053601 (2016).
- [36] S. P. Nolan, S. S. Szigeti, and S. A. Haine, Optimal and robust quantum metrology using interaction-based readouts, *Phys. Rev. Lett.* **119**, 193601 (2017).
- [37] S. A. Haine, Using interaction-based readouts to approach the ultimate limit of detection-noise robustness for quantum-enhanced metrology in collective spin systems, *Phys. Rev. A* **98**, 030303 (2018).
- [38] Q. Liu, L.-N. Wu, J.-H. Cao, T.-W. Mao, X.-W. Li, S.-F. Guo, M. K. Tey, and L. You, Nonlinear interferometry beyond classical limit enabled by cyclic dynamics, *Nature Physics* **18**, 167 (2022).
- [39] Q. Liu, T.-W. Mao, M. Xue, L.-N. Wu, and L. You, Cyclic nonlinear interferometry with entangled non-gaussian spin states, *Phys. Rev. A* **107**, 052613 (2023).
- [40] Z. Hu, Q. Li, X. Zhang, L.-G. Huang, H.-b. Zhang, and Y.-C. Liu, Spin squeezing with arbitrary quadratic collective-spin interactions, *Phys. Rev. A* **108**, 023722 (2023).
- [41] Z. Hu, Q. Li, X. Zhang, H.-b. Zhang, L.-G. Huang, and Y.-C. Liu, Nonlinear time-reversal interferometry with arbitrary quadratic collective-spin interaction, *Chinese Physics B* (2023).
- [42] O. Hosten, R. Krishnakumar, N. J. Engelsen, and M. A. Kasevich, Quantum phase magnification, *Science* **352**, 1552 (2016).
- [43] D. Linnemann, H. Strobel, W. Muessel, J. Schulz, R. J. Lewis-Swan, K. V. Kheruntsyan, and M. K. Oberthaler, Quantum-enhanced sensing based on time reversal of nonlinear dynamics, *Phys. Rev. Lett.* **117**, 013001 (2016).
- [44] S. C. Burd, R. Srinivas, J. J. Bollinger, A. C. Wilson, D. J. Wineland, D. Leibfried, D. H. Slichter, and D. T. C. Allcock, Quantum amplification of mechanical oscillator motion, *Science* **364**, 1163 (2019).
- [45] S. Colombo, E. Pedrozo-Penafiel, A. F. Adiyatullin, Z. Li, E. Mendez, C. Shu, and V. Vuletić, Time-reversal-based quantum metrology with many-body entangled states, *Nature Physics* **18**, 925 (2022).
- [46] S. Colombo, E. Pedrozo-Penafiel, and V. Vuletić, Entanglement-enhanced optical atomic clocks, *Applied Physics Letters* **121**, 210502 (2022).
- [47] T. Rosenband and D. R. Leibbrandt, [Exponential scaling of clock stability with atom number \(2013\)](#), [arXiv:1303.6357 \[quant-ph\]](#).
- [48] W. Li, S. Wu, A. Smerzi, and L. Pezzè, Improved absolute clock stability by the joint interrogation of two atomic ensembles, *Phys. Rev. A* **105**, 053116 (2022).
- [49] D. B. Hume and D. R. Leibbrandt, Probing beyond the laser coherence time in optical clock comparisons, *Phys. Rev. A* **93**, 032138 (2016).
- [50] J. Borregaard and A. S. Sørensen, Near-heisenberg-limited atomic clocks in the presence of decoherence, *Phys. Rev. Lett.* **111**, 090801 (2013).
- [51] D. Yankelev, C. Avinadav, N. Davidson, and O. Firstenberg, Atom interferometry with thousand-fold increase in dynamic range, *Science Advances* **6**, eabd0650 (2020).
- [52] A. L. Shaw, R. Finkelstein, R. B.-S. Tsai, P. Scholl, T. H. Yoon, J. Choi, and M. Endres, Multi-ensemble metrology by programming local rotations with atom movements, *Nature Physics* **20**, 195 (2024).
- [53] X. Zheng, J. Dolde, and S. Kolkowitz, Reducing the instability of an optical lattice clock using multiple atomic ensembles, *Phys. Rev. X* **14**, 011006 (2024).
- [54] S. Direkci, R. Finkelstein, M. Endres, and T. Gefen, Heisenberg-limited bayesian phase estimation with low-depth digital quantum circuits, [arXiv preprint arXiv:2407.06006 \(2024\)](#).
- [55] L.-Z. Liu, Y.-Y. Fei, Y. Mao, Y. Hu, R. Zhang, X.-F. Yin, X. Jiang, L. Li, N.-L. Liu, F. Xu, Y.-A. Chen, and J.-W. Pan, Full-period quantum phase estimation, *Phys. Rev. Lett.* **130**, 120802 (2023).
- [56] J. Zhou, J. Huang, J. Wei, C. Han, and C. Lee, [High-dynamic-range atomic clocks with dual heisenberg-limited precision scaling \(2024\)](#), [arXiv:2411.14944 \[quant-ph\]](#).
- [57] T. G. Thurtell and A. Miyake, Optimizing one-axis twists for variational bayesian quantum metrology, *Phys. Rev. Res.* **6**, 023179 (2024).
- [58] C. D. Marciniak, T. Feldker, I. Pogorelov, R. Kaubruegger, D. V. Vasilyev, R. van Bijnen, P. Schindler, P. Zoller, R. Blatt, and T. Monz, Optimal metrology with programmable quantum sensors, *Nature* **603**, 604 (2022).
- [59] C. Luo, H. Zhang, A. Chu, C. Maruko, A. M. Rey, and J. K. Thompson, [Hamiltonian engineering of collective xyz spin models in an optical cavity \(2024\)](#), [arXiv:2402.19429 \[quant-ph\]](#).
- [60] C. Miller, A. N. Carroll, J. Lin, H. Hirzler, H. Gao, H. Zhou, M. D. Lukin, and J. Ye, Two-axis twisting using floquet-engineered xyz spin models with polar molecules, *Nature* **633**, 332 (2024).
- [61] K. Macieszczak, M. Fraas, and R. Demkowicz-Dobrzański, Bayesian quantum frequency estimation in presence of collective dephasing, *New Journal of Physics* **16**, 113002 (2014).
- [62] E. Chitambar, D. Leung, L. Mančinska, M. Ozols, and A. Winter, Everything you always wanted to know about LOCC (but were afraid to ask), *Communications in Mathematical Physics* **328**, 303 (2014).
- [63] L. Pezzè and A. Smerzi, Heisenberg-limited noisy atomic clock using a hybrid coherent and squeezed state protocol, *Phys. Rev. Lett.* **125**, 210503 (2020).
- [64] D. J. Wineland, J. J. Bollinger, W. M. Itano, F. L. Moore, and D. J. Heinzen, Spin squeezing and reduced quantum noise in spectroscopy, *Phys. Rev. A* **46**, R6797 (1992).
- [65] D. J. Wineland, J. J. Bollinger, W. M. Itano, and D. J. Heinzen, Squeezed atomic states and projection noise in spectroscopy, *Phys. Rev. A* **50**, 67 (1994).
- [66] S. A. Haine and J. J. Hope, Machine-designed sensor to make optimal use of entanglement-generating dynamics for quantum sensing, *Phys. Rev. Lett.* **124**, 060402 (2020).
- [67] J. Huang, M. Zhuang, J. Zhou, Y. Shen, and C. Lee, Quantum metrology assisted by machine learning, *Advanced Quantum Technologies* **n/a**, 2300329.
- [68] S. A. Haine, Using interaction-based readouts to approach the ultimate limit of detection-noise robustness for quantum-

enhanced metrology in collective spin systems, [Phys. Rev. A](#) **98**, 030303 (2018).

[69] See supplemental information, contains additional figures and

details.

[70] J. Ye and P. Zoller, Essay: Quantum sensing with atomic, molecular, and optical platforms for fundamental physics, [Phys. Rev. Lett.](#) **132**, 190001 (2024).